On the Mechanism of Proton Transport by the Neuronal Excitatory Amino Acid Carrier 1

Natalie Watzke,* Thomas Rauen,‡ Ernst Bamberg,* and Christof Grewer*

From the *Max-Planck-Institut für Biophysik, D-60596 Frankfurt, Germany; and ‡Max-Planck-Institut für Hirnforschung, D-60528 Frankfurt, Germany

ABSTRACT Uptake of glutamate from the synaptic cleft is mediated by high affinity transporters and is driven by Na^+, K^+, and H^+ concentration gradients across the membrane. Here, we characterize the molecular mechanism of the intracellular pH change associated with glutamate transport by combining current recordings from excitatory amino acid carrier 1 (EAAC1)–expressing HEK293 cells with a rapid kinetic technique with a 100-μs time resolution. Under conditions of steady state transport, the affinity of EAAC1 for glutamate in both the forward and reverse modes is strongly dependent on the pH on the cis-side of the membrane, whereas the currents at saturating glutamate concentrations are hardly affected by the pH. Consistent with this, the kinetics of the pre–steady state currents, measured after saturating glutamate concentration jumps, are not a function of the pH. In addition, we determined the deuterium isotope effect on EAAC1 kinetics, which is in agreement with proton cotransport but not OH^- countertransport. The results can be quantitatively explained with an ordered binding model that includes a rapid proton binding step to the empty transporter followed by glutamate binding and translocation of the proton-glutamate-transporter complex. The apparent pK of the extracellular proton binding site is ~8. This value is shifted to ~6.5 when the substrate binding site is exposed to the cytoplasm.

KEY WORDS: glutamate transporter • patch-clamp • laser-pulse photolysis • rapid kinetics • reverse transport

INTRODUCTION

L-Glutamate is the major excitatory neurotransmitter in the mammalian brain (Kandel et al., 1995). After synaptic signal transmission, which is initiated by glutamate secretion into the synaptic cleft, extracellular glutamate is taken up into the neurons and glial cells surrounding the synapse. This process is mediated by high affinity glutamate transporters and allows these cells to maintain a 10^6-fold concentration gradient of glutamate across their plasma membrane (Zerangue and Kavanaugh, 1996a), which is essential for normal function of the nervous system. Such a high concentration gradient is thermodynamically possible because transport of each glutamate molecule is coupled to cotransport of three sodium ions and countertransport of one potassium ion down their electrochemical gradients (Kanner and Sharon, 1978; Wadiche et al., 1995a; Zerangue and Kavanaugh, 1996a).

Additionally, movement of a pH-changing ion is associated with glutamate transport because glutamate uptake mediates intracellular acidification (Erecinska et al., 1983; Bouvier et al., 1992; Zerangue and Kavanaugh, 1996a). However, the molecular mechanism underlying this pH change presently is not well understood. Initially, it was proposed that hydroxide is the pH-changing ion that is countertransported along with K^+ in the glutamate-independent transporter relocation step (Bouvier et al., 1992). However, based on the finding that, at physiological pH (7.4), the mainly neutral zwitterion cysteine is transported by the excitatory amino acid carrier 1 (EAAC1)[1] without concomitant intracellular pH change, Kavanaugh and colleagues proposed that a proton is cotransported with glutamate and three sodium ions in the initial charge translocation step (Zerangue and Kavanaugh, 1996a). These results allowed the conclusion that both the neutral (protonated) and the negatively charged forms of the substrate are recognized and transported by EAAC1 (Zerangue and Kavanaugh, 1996b). These findings raise the possibility that glutamate itself is the pH-changing species by being protonated at the γ-carboxylate group induced by a major pK change of this group after binding of the negatively charged substrate to the transporter (Slotboom et al., 1999). However, in terms of a kinetic mechanism, this interpretation would require a strict binding order of the substrates. Binding of negatively charged glutamate to the transporter occurs first, followed by protonation of the transporter–glutamate complex.

Recently, we introduced the method of laser-pulse photolysis of caged glutamate to investigate the pre–

Christof Grewer, Ph.D., Max-Planck-Institut für Biophysik, Kennedyallee 70, D-60596 Frankfurt, Germany. Fax: 49-69-6303-305; E-mail: christof.grewer@mpibp-frankfurt.mpg.de

[1]*Abbreviation used in this paper:* αCNB, α-carbonyl-2-nitrobenzyl; EAAC1, excitatory amino acid carrier 1; HEK, human embryonic kidney.

steady state kinetics of glutamate transporters with a time resolution in the 100-μs range (Grewer et al., 2000b). Analogous methods have been used in the past to study the molecular mechanism of various neurotransmitter receptors (Hess, 1993) and ion pumps (Fendler et al., 1985). Using this approach, we demonstrated that early steps in the reaction cycle of the neuronal glutamate transporter EAAC1 (Kanai and Hediger, 1992), such as glutamate translocation across the membrane, take place on a millisecond time scale, about an order of magnitude faster than steady state turnover of the protein. Rapid kinetic experiments are used in this study to investigate the mechanism of the pH change associated with glutamate transport in detail.

The results demonstrate that EAAC1 has to be protonated before glutamate binds at the extracellular side and charge translocation takes place. This implies the existence of an ionizable amino acid residue in the protein with an apparent pK of 8 that is responsible for proton cotransport. The dissociation of glutamate on the intracellular side of the transporter is controlled by a pK shift of this residue by at least 1.5 pK units that takes place after glutamate translocation.

MATERIALS AND METHODS

Expression of EAAC1 in Mammalian Cells

EAAC1 cloned from rat retina (Rauen et al., 1996; Grewer et al., 2000b) was subcloned into the vector pBK-CMV (Stratagene) and used for transient transfection of subconfluent human embryonic kidney cell (HEK293; ATCC No. CGL 1573) cultures with the calcium phosphate–mediated transfection method as previously described (Chen and Okayama, 1987). Electrophysiological recordings were performed during the first 3 d after transfection.

Electrophysiology

Glutamate-induced EAAC1 currents were recorded with an amplifier (model EPC7; Adams & List) under voltage-clamp conditions either in the whole-cell current-recording configuration or in the inside-out patch-clamp configuration (Hamill et al., 1981). The typical resistance of the recording electrode was 2–3 MΩ (whole-cells) or 300–400 kΩ (inside-out giant patches). EAAC1-associated currents are composed of two components, a coupled transport current and an uncoupled current carried by anions termed $I^{Glu^-}_{Na^+/K^+}$ and $I^{Glu^-}_{anionic}$, respectively (Fairman et al., 1995; Wadiche et al., 1995b; Otis and Jahr, 1998). Two different pipette solutions were used depending on whether $I^{Glu^-}_{anionic}$ (with thiocyanate) or $I^{Glu^-}_{Na^+/K^+}$ (with chloride) was investigated (in mM): 130 KSCN or KCl, 2 $MgCl_2$, 10 TEACl, 10 EGTA, and 10 HEPES (pH 7.4, KOH). The addition of 2.5 mM $CaCl_2$ (<0.1 μM of free calcium) had no influence on the detected current. The external solution contained the following (in mM): 140 NaCl, 2 $MgCl_2$, 2 $CaCl_2$, 15 Tris, and 15 Mes (pH 6.0, 7.0, 7.4, 8.0, and 9.0; HCl or NaOH), 30 CAPS (pH 10.0, NaOH), or 15 Tris and 15 sodium succinate (pH 4.8, HCl). If high glutamate concentrations (≥5 mM) were used, the nonactivating bath solution contained additional amounts of Tris (up to 8 mM) to balance the osmolarity. The same solutions were used for the reverse transport studies. To avoid the formation of vesicles in the inside-out patch configuration, the pipette solution contained no $CaCl_2$ (Hamill et al., 1981). All of the experiments were performed at room temperature. In the case of the D_2O experiments, the buffer components were dissolved in D_2O instead of H_2O (pD 7.7). Each experiment was repeated at least five times with at least three different cells/patches and the error bars represent the error of the single measurement and not the error of the mean (mean ± SD).

Laser-pulse Photolysis and Rapid Solution Exchange

The rapid solution exchange (time resolution ~100 ms) was performed with a quartz tube (inner diameter 350 μm) positioned 0.5 mm from the cell. The linear flow rate of the solutions emerging from the opening of the tube was ~5–10 cm/s. Laser-pulse photolysis experiments were performed as described previously (Niu et al., 1996). α-Carbonyl-2-nitrobenzyl (αCNB)–caged glutamate (Molecular Probes) in concentrations of 1 mM (pH 6.0 and 7.4) to 4 mM (pH 9.0) or free glutamate was applied to the cells, and photolysis of the caged glutamate was initiated with a light flash (340-nm, 15-ns excimer laser pumped dye laser; Lambda Physik). The light was coupled into a quartz fiber (diameter, 365 μm) that was positioned in front of the cell in a distance of 300 μm. With maximum light intensities of 500–600 mJ/cm², saturating glutamate concentrations could be released, which were tested by comparing the photolysis-induced steady state current with that generated by rapid perfusion of the same cell with 100 μM glutamate (pH 6.0 and 7.4) or 500 μM glutamate, pH 9.0 (Grewer, 1999).

Data were recorded using the pClamp6 software (Axon Instruments), digitized with a sampling rate of 1 kHz (solution exchange) or 25 kHz (laser-pulse photolysis) and low pass–filtered at 250 Hz or 3 kHz, respectively. Nonlinear regression fits of experimental data were performed with Origin (Microcal software) or Clampfit (pClamp8 software; Axon Instruments).

RESULTS

The basic experiments on the effect of pH on EAAC1 expressed in HEK293 cells are shown in Fig. 1 D (right), demonstrating results that differ from those reported by Billups and Atwell (1996) for native glutamate transporters in Müller cells. Namely, EAAC1-associated currents induced by a constant concentration of 125 μM glutamate are reduced only at basic pH; but, in contrast to the Müller cell transporters, they are not reduced in the acidic pH range. To understand this different behavior, we investigated the mechanism of the proton translocation process by EAAC1 in more detail.

pH Dependence of the K_M for Glutamate

In the following experiments the highly permeant anion SCN^- was used as the main intracellular anion to increase transporter-associated currents (Wadiche et al., 1995a). First, we determined the effect of the pH on the apparent affinity of EAAC1 for glutamate under steady state conditions. In the forward transport mode this was performed using rapid solution exchange combined with whole-cell recordings of HEK_{EAAC1} cells voltage-clamped to 0 mV, and keeping the intracellular pipette solution at a constant pH of 7.4. Although currents were larger at negative transmembrane potentials, we used 0 mV because current recordings were, in

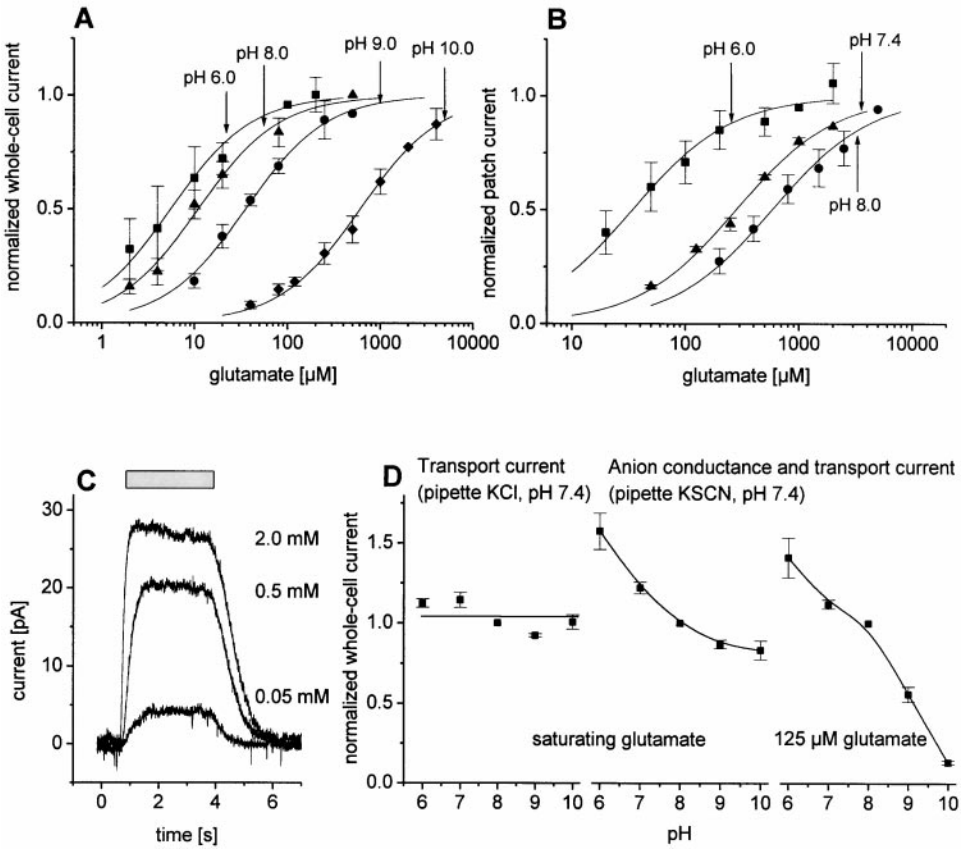

FIGURE 1. (A) pH dependence of the apparent K_M for glutamate from whole-cell current recordings with a KSCN-based pipette solution (pH internal = 7.4) under steady state conditions. Glutamate was applied to the cell with a rapid solution exchange device. The solid lines represent fits of the Hill equation $I = (I_{max} \cdot [\text{glutamate}]^n)/(K_M + [\text{glutamate}])^n$, with a Hill coefficient of n = 1, to the experimental data at pH 6.0 (square), 8.0 (triangle), 9.0 (circle), and 10.0 (diamond) (all error bars represent mean ± SD). The whole-cell currents were normalized to I_{max}. The transmembrane potential was 0 mV. In contrast to the excised patches, the whole-cell current recordings became quite unstable at an extracellular pH of 5 and below. Therefore, such low pH values were avoided in the forward transporter mode. (B) pH dependence of the apparent K_M for glutamate on the intracellular side in the reverse transport mode. The solid lines represent fits of the Hill equation (same as A) with n = 1 to the experimental data at pH 6.0 (square), 7.4 (triangle), and 8.0 (circle), (all error bars represent mean ± SD). The inside-out patch currents were normalized to I_{max}. The transmembrane potential was 0 mV. The extracellular pH was 7.4. (C) Typical current recordings form an inside-out HEK_{EAAC1} patch (V = 0 mV) under reverse transport conditions, where glutamate in concentrations of 0.05, 0.5, and 2 mM was applied at the indicated times (bar) with a solution exchange device. Leak currents were subtracted and a KSCN-based pipette solution was used. The extra- and intracellular pH was 7.4. (D) Effect of pH on I_{max}. (Left) Steady state forward transport currents from voltage-clamped HEK_{EAAC1} whole-cells were measured at different pH values induced by rapid application of saturating glutamate concentrations (12-fold K_M). The conditions of the experiment were as follows: KCl-based pipette solution, a NaCl-based bath solution, and a holding potential of 0 mV. (Middle) Whole-cell current recordings from voltage-clamped HEK_{EAAC1} cells (V = 0 mV) at different pH values induced by saturating glutamate concentrations (12-fold K_M). The solid line was drawn by eye. With the use of a KSCN-based pipette solution, the detected currents mainly result from anion conductance ($I^{Glu^-}_{anionic}$). (Right) Same as in the middle trace but with a constant glutamate concentration of 125 μM. The whole-cell currents were normalized to the glutamate current at pH 8.0, and the solid line was drawn by eye.

general, more stable under these conditions. The glutamate concentration dependencies of the whole-cell current at external pH values from 6.0 to 10.0 are shown in Fig. 1 A and followed Michaelis-Menten–like relationships throughout the whole pH range studied. The apparent affinity of EAAC1 for glutamate (K_M) was almost unaffected between pH 6.0 and 8.0 (Fig. 1 A). However, raising the pH above 8.0 increased the K_M from 11 μM at pH 8.0 to 610 μM at pH 10.0 (Table I), which is in line with findings of Erecinska and co-workers (1983) for D-aspartate uptake in brain synaptosomes.

Subsequently, the pH dependence was examined in the reverse transport mode under conditions of steady state transport by using the patch-clamp technique in the inside-out configuration (Hamill et al., 1981). As shown in Fig. 1 (B and C) currents from a HEK_{EAAC1}-excised inside-out patch (V = 0 mV), induced by increasing glutamate concentrations at a symmetrical pH of 7.4 on both sides of the membrane, revealed a K_M value of 280 μM, which is 40-fold higher than the K_M of EAAC1 for extracellular glutamate in the forward transport mode. However, this affinity shift of the transporter could be partially reversed by increasing the intracellular proton concentration 25-fold. Under these conditions, the apparent K_M decreases from 280 μM at pH 7.4 to 34 μM at pH 6.0 (Fig. 1 B). On the other hand, a fourfold decrease of the intracellular proton concentration, pH 8.0, leads to an increase of the apparent K_M to 580 μM, suggesting that proton binding on the intracellular as well as on the extracellular side of EAAC1 exhibits qualitatively a similar pH depen-

TABLE I

pH Dependence of EAAC1 Affinity for Glutamate

pH	Extracellular K_m	n	Intracellular K_m	n
	μM		μM	
4.8			820 ± 70	4
6.0	5.8 ± 0.7	6	34 ± 5	10
7.0	9.4 ± 1.8	4		
7.4	5.9 ± 1.3	10	280 ± 30	8
8.0	11 ± 1	9	580 ± 90	8
9.0	36 ± 3	8		
10.0	610 ± 50	10		
	580 ± 80*	5		

Apparent affinity of EAAC1 for glutamate at the extra- and intracellular side as a function of pH. The pipette solution contained thiocyanate. *n*, number of independent determinations. *Transport current.

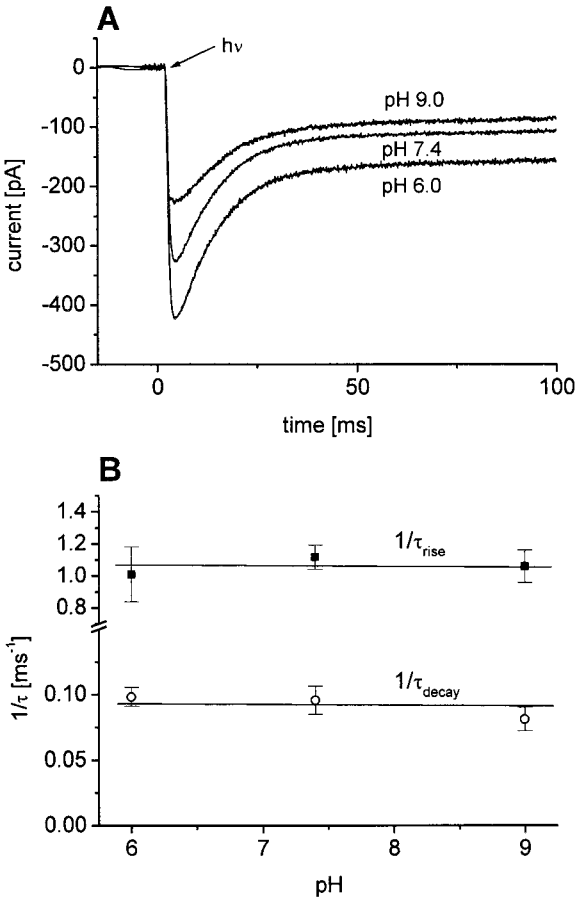

FIGURE 2. (A) Laser-pulse photolysis experiments of αCNB-caged glutamate on a single cell at different pH values with a KSCN-based pipette solution at V = 0 mV. Photolysis was initiated by a laser flash at t = 0. Leak currents were subtracted, and the steady state currents were normalized. The experimental data were fitted to the following equation: $I = I_1 \cdot \exp(-t/\tau_{decay}) + I_2 \cdot \exp(-t/\tau_{rise}) + I_{ss}$, where I_{ss} represents the steady state current. Parameters are as follows: for pH 6.0 and 7.4, 1 mM caged glutamate, ≈125 μM released glutamate, τ_{rise} 0.77 ± 0.01 ms and 0.81 ± 0.01 ms, respectively, and τ_{decay} 10.7 ± 0.1 ms and 10.8 ± 0.1 ms, respectively; and for pH 9.0, 4 mM, ≈500 μM released glutamate, τ_{rise} 0.94 ± 0.02 ms, and τ_{decay} 12.9 ± 0.1 ms. (B) Averaged values (mean ± SD) for $1/\tau_{rise}$ (squares) and $1/\tau_{decay}$ (circles) of three different cells as shown in A at pH 6.0, 7.4, and 9.0, respectively. $1/\tau_{rise}$ 1.0 ± 0.2 ms^{-1}, 1.1 ± 0.1 ms^{-1}, and 1.1 ± 0.1 ms^{-1}; $1/\tau_{decay}$ 98 ± 7 s^{-1}, or 95 ± 10 s^{-1}, and 81 ± 9 s^{-1}.

dence. However, the pH dependence on the intracellular side is shifted by at least 1.5 pH units to the acidic range. At very low pH values of 4.8, when ~30% of the glutamate is protonated (pK 4.4), the affinity for glutamate once again decreases dramatically and reaches a K_M of 820 μM (Table I). To exclude that this effect is due to the increased ionic strength imposed by the succinate-Tris buffer, the apparent K_M for glutamate at pH 7.4 in the forward transport mode was determined in the presence of succinate-Tris buffer, showing no difference to the results obtained with a Mes-Tris buffer.

It has been reported previously that the apparent K_M of glial transporter subtypes for glutamate at pH 7.3 does not change depending on whether the uncoupled anion current($I^{Glu^-}_{anionic}$) or exclusively the coupled transport current ($I^{Glu^-}_{Na^+/K^+}$) is measured (Mennerick et al., 1999). Consistent with this, at pH 10.0, where the largest K_M change was observed, the apparent K_M values determined with symmetrical chloride concentrations (610 ± 50 μM, $I^{Glu^-}_{anionic}$) and with intracellular thiocyanate (580 ± 80 μM, $I^{Glu^-}_{Na^+/K^+}$) are similar. This result demonstrates that the change of the apparent affinity for glutamate at high pH values represents an intrinsic property of the EAAC1 and is not caused by a pH dependence of only the anion-conducting state.

pH Dependence of the Glutamate-induced Current I_{max}

To investigate the binding sequence of the proton and glutamate to the transporter, the maximum currents (I_{max}) at saturating glutamate concentrations were compared in a pH range between 6.0 and 10.0. These experiments were performed by measuring $I^{Glu^-}_{Na^+/K^+}$ in the whole-cell current recording configuration of voltage-clamped HEK_{EAAC1} at 0 mV. As shown in Fig. 1 D (left), I_{max} does not depend significantly on the proton concentration under these conditions. This kind of analysis allows the direct experimental determination of the proton–glutamate binding sequence: the fact that I_{max} is not affected by the pH indicates that proton binding occurs first, followed by glutamate binding. The pH effect on $I^{Glu^-}_{anionic}$ was also determined. In contrast to $I^{Glu^-}_{Na^+/K^+}$, the glutamate-induced anionic currents exhibit a pH dependence, showing a moderate increase of $I^{Glu^-}_{anionic}$ with decreasing pH (Fig. 1 D, middle).

Finally, to test if the pH dependence is qualitatively similar in the reverse transport mode, the same experiments were performed using inside-out patches excised from HEK_{EAAC1}. Consistent with the results obtained in the forward transport mode, a slight pH dependence

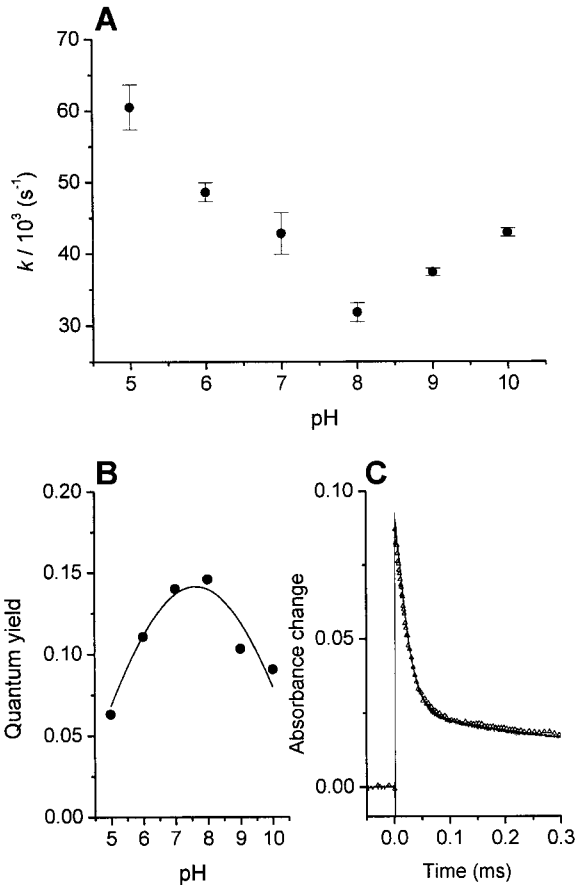

FIGURE 3. (A) Rate constant of the *aci*-nitro intermediate decay of αCNB-caged glutamate as a function of the pH of the solution. The buffer solutions were as follows: acetate (pH 5), phosphate (pH 6, 7, and 8), and borate (pH 9 and 10) at concentrations of 100 mM. The temperature of the experiments was 22°C. A solution of 500 μM αCNB-caged glutamate in a quartz cuvette (2 × 10–mm path length; Hellma) was excited by a laser light pulse of 308-nm wavelength and 10-ns pulse duration (∼50 mJ energy/pulse; model EMG200; Lambda Physics). The absorption change after laser excitation was monitored perpendicular to the laser beam with the light of a Xenon lamp. The wavelength of the analysis light was selected with a monochromator (The Optometrics Group) and was 430 nm. The light intensity as a function of time was measured with a PIN photodiode (Siemens). The signal of the photodiode was preamplified (model PMT-4; Advanced Research Instruments), recorded with a digital oscilloscope (model 9310AM; LeCroy), and stored on a floppy disk. The rate constants were evaluated by fitting a double exponential decaying function to the *aci*-nitro intermediate absorbance with the Origin software (MicroCal). The error bars represent ± SD (n = 3). (B) pH dependence of the quantum yield of αCNB-caged glutamate photolysis. The conditions of the experiments were as described in A. The quantum yield was determined as previously described (Grewer et al., 2000a) by measuring the absorbance (A_n) of the *aci*-nitro intermediate as a function of the number of consecutive laser pulses (n) assuming that (a) the absorbance and, therefore, the concentration of the *aci*-nitro intermediate is directly proportional to the concentration of the liberated glutamate; and (b) the absorbance of the solution is not dependent on n (irradiation near the isosbestic point; Milburn et al., 1989; Grewer et al., 2000a). The quantum yield ϕ was determined by linear regression analysis after plotting $\ln(A_n)$ versus $(n - 1)$ (Milburn et al., 1989). (C) Time dependence of the *aci*-nitro intermediate absorbance in H_2O-based (triangles, pH 7.0) and D_2O-based (solid line, pD 7.3). The buffer was 100 mM phosphate and the analysis wavelength was 440 nm. The concentration of αCNB-caged glutamate was 200 μM. The 308-nm laser was flashed at t = 0. The other conditions of the experiment were the same as in A.

was also observed for $I^{Glu^-}_{anionic}$. Compared with the current at pH 8.0, which was induced by saturating glutamate concentrations, I_{max} for pH 7.4 and 6.0 was 1.13 ± 0.04 (n = 3) and 1.27 ± 0.03 (n = 3), respectively.

Effect of Proton Concentration on Pre–steady State Kinetics of EAAC1

The laser-pulse photolysis method of caged glutamate was used to determine the pH effect on the pre–steady state kinetics of EAAC1 and resolved a rapid transient current component preceding the steady state current in the presence of thiocyanate in the pipette (1 mM caged glutamate, ≈125 μM released glutamate; Fig. 2 A, middle trace). The transient current results from the rapid synchronized formation of a glutamate-gated anion-conducting state that is followed by the subsequent population of other transporter states (desynchronization of the transporters) as it approaches a new steady state (Wadiche and Kavanaugh, 1998; Grewer et al., 2000b; Otis and Kavanaugh, 2000). At pH 7.4 and 0 mV transmembrane potential, this decay proceeds with a time constant of 10.5 ± 1.2 ms (n = 3), which is consistent with a previous report (Grewer et al., 2000b).

Assuming that the glutamate binding follows the proton binding step and proton binding is fast, the pre–steady state kinetics of EAAC1 should not be affected by pH changes at saturating glutamate concentrations. In contrast, if glutamate binds first to the transporter and the proton binding step follows subsequently, the rate of formation of the proton-glutamate-transporter complex should depend on the proton concentration. Furthermore, at low proton concentrations, it is expected that this would slow down the rise and decay time for the transient current, even if the glutamate concentration is saturating. To differentiate between these two possibilities, the pre–steady state currents upon photolytic release of saturating glutamate concentrations were monitored additionally at pH 6.0 and 9.0 (≈500 μM released glutamate) as shown in Fig. 2 A. Despite the small change in the current amplitude, which was already observed under conditions of steady state transport, the pre–steady state kinetics of EAAC1 are not substantially altered and are not pH-dependent. Consistent with this, the time constants for the formation and the decay of the transient current component are not significantly influenced by the pH (Fig. 2 B), indicating that the pH specifically affects EAAC1

proton transport, but not the kinetics and function of EAAC1 by unspecific effects, within the pH range examined. Photolytic release of subsaturating concentrations of glutamate at pH 9.0, however, leads to reduced rates for the formation and deactivation of the transient current (not shown). This effect is indistinguishable from that observed at pH 7.4, but its dose dependence is shifted to higher glutamate concentrations.

To test if the photolysis rate of caged glutamate, which is known to be pH-dependent from analogous compounds (Milburn et al., 1989; Grewer et al., 2000a), is sufficient for the time-resolved measurements of the pre–steady state currents throughout the pH range studied, we performed the following control experiments. A short-lived intermediate in the αCNB-caged compound photolysis reaction, the *aci*-nitro intermediate, has a characteristic absorption at 430 nm and its decay kinetics are commonly accepted to represent the release kinetics of the caged substrate (Walker et al., 1988). At pH 7.0, the *aci*-nitro intermediate decays with a time constant of 23 ± 1 μs ($n = 5$), in agreement with a previous report (Wieboldt et al., 1994). The pH dependence of this time constant is shown in Fig. 3 A. The decay rate increases at both low and high pH values with a minimum at pH 8.0, indicating that the photolytic release of glutamate is not rate limiting for the EAAC1 reaction processes. At pH 9.0, where the laser-pulse photolysis experiments with EAAC1 were performed in general, the photolysis rate constant of 38,000 s^{-1} is ~40 times faster than the rise of the whole-cell current in the transient kinetic experiment (Fig. 2 A). In addition, the photolysis quantum yield (ϕ) was measured as a function of the pH, as shown in Fig. 3 B. The quantum yield is slightly pH-dependent, exhibiting a maximum between pH 7 and 8. At pH 9.0 ($\phi = 0.1$, $n = 3$) it has 71% of its value at pH 7.0 ($\phi = 0.14$; Wieboldt et al., 1994). These data indicate that over the whole pH range studied, the photolysis quantum yield is sufficient to photolytically release saturating concentrations of glutamate.

pH Effect on Current–Voltage Relationships of EAAC1

So far, the data were collected at 0 mV transmembrane potential and they are consistent with an ordered binding sequence of the proton, followed by glutamate to the transporter. Furthermore, the data indicate that even at a proton concentration of 0.1 nM, pH 10, protonation is not rate limiting for the overall turnover of the transporter, as demonstrated by the kinetic experiments. To test if this is also correct at different transmembrane potentials, the influence of the pH on the voltage dependence of steady state EAAC1 currents was determined. The voltage dependence of the steady state $I^{Glu^-}_{Na^+/K^+}$ current (symmetrical Cl^- on both sides of the membrane) at pH 7.4 is shown in Fig. 4 A. Consistent with previous results, this current is inwardly directed, increases with decreasing transmembrane potential, and does not reverse within the voltage range studied. This is typical for $I^{Glu^-}_{Na^+/K^+}$ of EAAC1 and generally observed under these ionic and pH conditions (Grewer et al., 2000b). At different pH values (from 6.0 to 9.0) the current–voltage relationship is basically unchanged as shown in Fig. 4 A. Identical experiments performed for $I^{Glu^-}_{anionic}$ in the presence of intracellular SCN^- (Fig. 4 B) demonstrate that the current is inwardly directed over the whole voltage range and the I–V curves are not affected by the pH. These results indicate that even at strongly negative transmembrane potentials, which accelerate the charge translocation steps with respect to other steps in the transport cycle (e.g., nonvoltage-dependent reactions), the turnover rate of the transporter is not changed by the pH. Therefore, proton binding does not become rate limiting.

The voltage dependence of the reverse transport mode of EAAC1, at pH of 7.4 on both sides of the membrane, was weaker than that of the forward transport mode (Fig. 4, C and D), which is consistent with previous results reported by Noda et al. (1999) and Szatkowski et al. (1990) using native transporters of unknown subtype composition. Similar results were obtained at an intracellular pH of 6.0 (data not shown).

Deuterium Kinetic Isotope Effect

Since it is proposed that glutamate transport is associated with the cotransport of a proton rather than a OH^- countertransport, we examined the deuterium isotope effect on the steady state and pre–steady state kinetics of EAAC1. Fig. 5 A compares whole-cell current recordings from a voltage-clamped HEK_{EAAC1} cell exposed to either a D_2O-based or a H_2O-based bath solution. The steady state glutamate-induced current is reduced by ~20% in the presence of D_2O compared with H_2O, indicating that the steady state turnover of EAAC1 is slightly slowed. To test which step in the transport cycle is affected by the solvent isotope substitution, we performed time-resolved measurements of the transient current component, which are shown in Fig. 5 B, for two different voltage-clamped HEK_{EAAC1} cells. Whereas the time constant of the rising phase is not affected by the substitution of D_2O for H_2O (0.91 ± 0.07 ms instead of 0.90 ± 0.06 ms with H_2O), the time constant of the decaying phase is increased from 10.5 ± 1.2 ms in the presence of H_2O to 18.3 ± 2.0 ms in the presence of D_2O (Fig. 5 C). These results indicate that mainly initial, rapid transporter reaction steps are affected by the solvent isotope substitution.

To determine if the rate constant and the quantum yield of caged glutamate photolysis are sensitive to substitution of D_2O for H_2O, we performed the control experiments shown in Fig. 3 C. Neither the amplitude nor

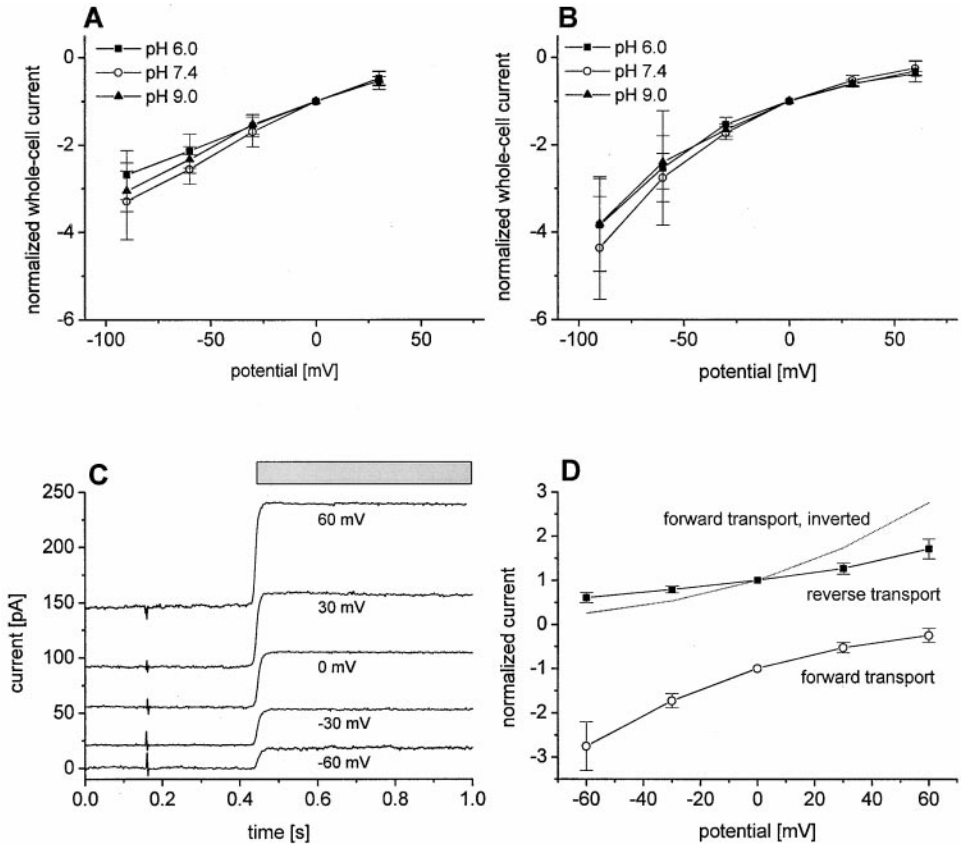

FIGURE 4. (A) Current-voltage relationships of glutamate-induced (concentration of 12-fold K_M) whole-cell currents under stationary conditions at pH 6.0 (solid square), 7.4 (open circle), and 9.0 (solid triangle), (mean ± SD), under SCN^--free conditions, measuring mainly the transport current $I^{Glu^-}_{Na^+/K^+}$. (B) Current-voltage relationships of glutamate-induced (concentration of 12-fold K_M) whole-cell currents at pH 6.0 (solid square), 7.4 (open circle), and 9.0 (solid triangle), (mean ± SD), measuring mainly the anion conductance ($I^{Glu^-}_{anionic}$) with a KSCN-based pipette solution (pH internal = 7.4). The whole-cell currents were normalized to the glutamate-induced current at a transmembrane potential of 0 mV. (C) Glutamate-induced (4 mM, indicated by bar) current recordings from an inside-out HEK_{EAAC1} patch at holding potentials of 60 to −60 mV in 30-mV increments (baseline adjusted) with pH 7.4 on the extracellular and intracellular side and a KSCN-based pipette solution. (D) Current-voltage relationships of $I^{Glu^-}_{anionic}$ under forward (whole-cell, open circles) and reverse (inside-out patch, solid squares) transport conditions ($n = 8$), normalized to the glutamate-induced current at a transmembrane potential of 0 mV, (mean ± SD). The I–V curve from the forward transport was inverted (dotted line) for better visualization.

the decay rate constant of the *aci*-nitro intermediate absorbance changed when H_2O was replaced by D_2O, suggesting the absence of a solvent isotope effect on αCNB-caged glutamate photolysis.

DISCUSSION

The results presented here provide new insights into the molecular mechanism of proton transport by glutamate transporters. Considering that the formation of a transporter-proton-glutamate complex is necessary for translocation in general, several different kinetic models are possible: (a) the transporter is protonated first, and then glutamate binding takes place (THS); (b) the glutamate anion binds first to the glutamate transporter and the proton binding step follows (TSH); (c) only the protonated form of glutamate is accepted by the transporter, or binding of the proton and glutamate is simultaneous (SHT/SHT-sim); and (d) the binding order of glutamate and the proton is sequential but random (THS/TSH). The models are listed in Table II together with the kinetic equations that quantitatively describe K_M and I_{max} as a function of the pH, and they are illustrated in Fig. 6 (A and B). For the derivation of these equations, we assumed that, in saturating concentrations of extracellular sodium and intracellular potassium, the turnover number of EAAC1 only depends on the population of the transporter in the state where all of the extracellular ligands are bound (three sodium ions, one proton, and one glutamate anion; Zerangue and Kavanaugh, 1996a), and that proton binding is in rapid preequilibrium with respect to glutamate translocation.

Using these prerequisites, the predictions of the models are directly comparable with our experimental results. The models TSH and THS/TSH predict that I_{max} decreases with increasing pH (Fig. 6 B), which is not consistent with our data. Therefore, these models can be excluded. For the same reason, we can also exclude that proton binding is rate limiting for the transporter turnover (Table II, THS slow binding). In contrast, I_{max} is pH-independent for the other three models. However, models SHT and SHT-sim predict that $\log(K_M)$ is a linear function of the pH (Fig. 6 A). This type of behavior is not found experimentally, allowing us to discard these models. The only mechanism that is in agreement with all the results is THS, assuming that proton

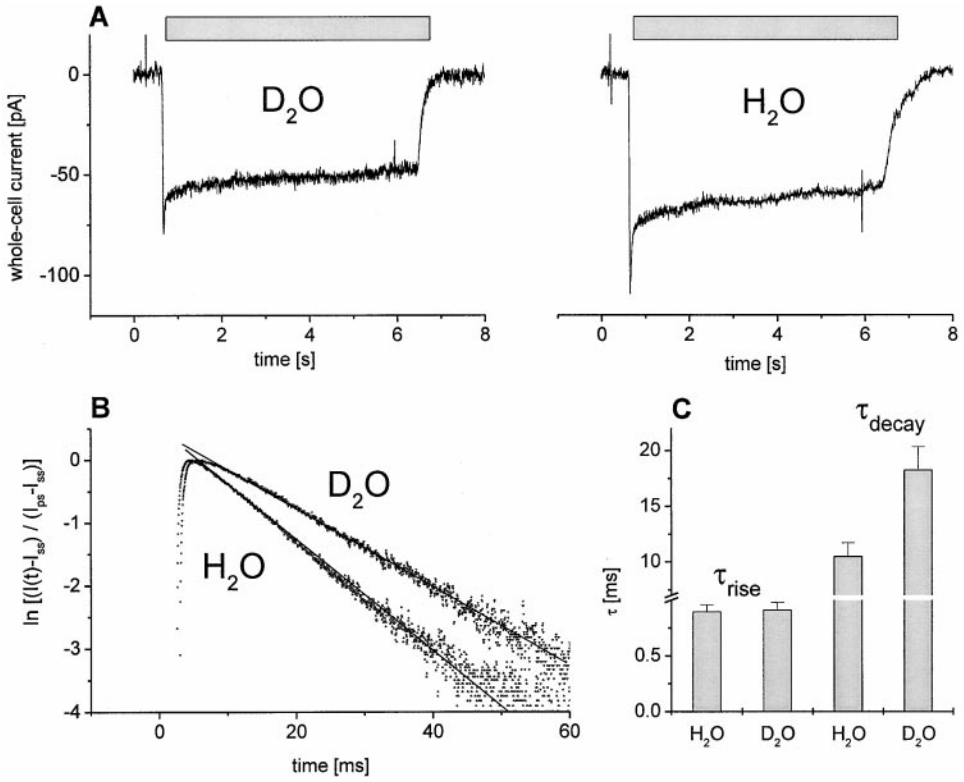

FIGURE 5. (A) Kinetic isotope effect. Whole-cell current recordings from one voltage-clamped HEK_{EAAC1} cell (V = 0 mV) with an internal solution containing SCN^-. The left panel shows the glutamate-induced current in a D_2O-based bath solution and, in comparison, the same experiment with a H_2O-based bath solution. Leak currents were subtracted. The EAAC1 current response to glutamate in the H_2O-based experiment was the same before and after D_2O replacement. (B) Laser-pulse photolysis experiments of αCNB-caged glutamate on two different cells in a D_2O- or H_2O-based bath solution with a pipette solution containing KSCN (V = 0 mV). Leak currents were subtracted, and the current was inverted and linearized with the formula $\ln[(I(t) - I_{ss})/I_{ps} - I_{ss})]$, where I_{ss} represents the steady state current and I_{ps} represents the pre–steady state current. With this type of plot, the rate constant for the transient decay is obtained with linear regression analysis from the slope of the curve. Parameters are as follows: for H_2O-based bath solution (pH 7.4), 1 mM caged glutamate, ≈125 μM of released glutamate, τ_{rise} 0.81 ± 0.01 ms, and τ_{decay} 10.8 ± 0.1 ms; and for D_2O-based bath solution (pD 7.7), 1 mM caged glutamate, ≈125 μM of released glutamate τ_{rise} 1.01 ± 0.01 ms, and τ_{decay} 16.5 ± 0.1 ms. (C) Averaged values (mean ± SD) for τ_{rise} and τ_{decay} of three different cells are as shown in B with H_2O or D_2O. τ_{rise} 0.90 ± 0.06 ms or 0.91 ± 0.07 ms, respectively; τ_{decay} 10.5 ± 1.2 ms or 18.3 ± 2.0 ms, respectively.

binding is fast compared with the transporter turnover. This model is shown in Fig. 6 D and correctly predicts that low proton concentrations can be compensated by high glutamate concentrations to fully restore transporter functionality. For this reason, the I_{max} induced by saturating glutamate concentrations does not depend on the pH. This effect is caused by a stabilization of the protonated form of the transporter upon glutamate binding. Furthermore, the model quantitatively accounts for the weak pH dependence found for the affinity of the transporter for glutamate between pH 6.0 and 8.0 as well as for the drastic increase in K_M between pH 8.0 and 10.0. Fitting this model to the extracellular K_M values, the pK of the ionizable amino acid residue on the transporter protein can be estimated to be ~8.0 in the absence of glutamate (Fig. 6, A and C). This pK is shifted to more basic values after glutamate binding takes place.

The pK for activation by protons estimated here represents an apparent value that incorporates the following: (a) other rate and equilibrium constants of ion-binding processes on the extracellular side, such as the Na^+ binding reaction that we omitted here for the sake of simplicity; and (b) local pH differences related to surface charge effects. The nature of the amino acid residue that binds the proton is unknown. Others (Zhang et al., 1994) have suggested that histidine 326 of the analogous glutamate transporter GLT-1, which is also conserved in EAAC1, is involved in proton binding.

Based on predictions of the THS model, the decay rate constant of the transient current component, $1/\tau_{decay}$ (Table II), is pH-independent at saturating glutamate concentrations (Fig. 2 B), whereas $1/\tau_{decay}$ decreases at nonsaturating glutamate concentrations, but with a pH-dependent K_M (Table II). All of the predictions drawn from the THS model are in line with our experimentally determined data. Furthermore, at saturating glutamate concentrations, extracellular proton binding does not become rate limiting for the turnover of the transporter or the glutamate translocation step, even at a proton concentration as low as 1 nM. Moreover, the lack of a proton effect on the rate constant of the current rise indicates that protonation of the transporter is not rate limiting for glutamate binding as well. However, this hypothesis requires comparatively high exchange rates of the proton binding residue with protons in the bulk solution or with buffer molecules with a pseudofirst-order rate constant of at least 1,000 s^{-1}. Typical rate constants

TABLE II

Kinetic Modeling of EAAC1 pH Dependence

Model	K_m	I_{max}	$1/\tau_{decay}$
THS	$\frac{K_s(K_H + [H])}{[H]}$	$\neq f([H])$	$\frac{[S]}{K_M + [S]} \cdot k_f + k_b \neq f([H])$
THS slow binding	$\frac{K_s[H]}{[H] + K_H}$	$\frac{[H]}{K_H + [H]}$	
TSH	$\frac{K_s K_H}{K_H + [H]}$	$\frac{[H]}{K_H + [H]}$	$\frac{[H]}{K_H + [H]} \cdot \frac{[S]}{K_M + [S]} \cdot k_f + k_b = f([H])$
SHT/SHT-sim	$\frac{K_s K_H}{[H]} / \frac{K_{HS}}{[H]}$	$\neq f([H])$	$\frac{[S]}{K_M + [S]} \cdot k_f + k_b \neq f([H])$
THS/TSH	$\frac{K_{S2}(K_H + [H])}{[H] + K_H K_{S2}/K_{S1}}$	$\frac{[H]}{[H] + K_H K_{S2}/K_{S1}}$	$\frac{[H]}{K_H \frac{K_{S2}}{K_{S1}} + [H]} \cdot \frac{[S]}{K_M + [S]} \cdot k_f + k_b = f([H])$

Kinetic equations for models of EAAC1 glutamate–proton cotransport. The following assumptions were made for K_M and I_{max}: (1) that translocation proceeds from the fully loaded carrier; and (2) that proton binding is very fast compared with steady state turnover, except for THS model slow binding. For the derivation of the equations for $1/\tau_{decay}$, we additionally assumed that glutamate binding is in rapid preequilibrium. For an explanation of the variables see Fig. 6. The indices 1 and 2 in the model THS/TSH denote binding of glutamate to the T and the TH state, respectively. In the case of simultaneous binding of glutamate and the proton to the transporter (STH-sim.), K_{HS} has the unit molar squared.

of proton transfer in aqueous solution are in the range of 10^7–10^{11} $M^{-1}s^{-1}$ (Eigen and Hammes, 1963), which is sufficient to explain the rapid proton transfer rates observed here even at pH 9.0.

What happens when glutamate is translocated across the membrane and the glutamate and proton binding sites are exposed to the cytoplasm? Both, the data obtained in the forward transport mode and in the reverse mode (K_M and I_{max}) are in the pH range of 6.0–8.0, which is compatible with a kinetic model that is based on an initial proton binding step of the empty transporter that is followed by glutamate binding, suggesting that the general mechanism of proton transport is similar for forward and reverse transport (Fig. 6 D). However, at physiological pH, the apparent affinity for glutamate is reduced ~40-fold under reverse transport conditions compared with the forward transport mode, suggesting that the glutamate transporter is asymmetric with respect to its kinetic properties (Nelson et al., 1983). In the absence of any pH gradient across the membrane, this is an important feature as the intracellular affinity for the substrate controls glutamate dissociation after translocation. However, this difference in substrate affinity between the two transport modes can partially be overcome by increasing the intracellular proton concentration to 1 μM, pH 6.0, indicating that, similar to the forward transport, the glutamate binding step is regulated by pH. Therefore, it seems likely that the intrinsic affinity of EAAC1 for glutamate is not substantially different between the forward and reverse transport modes, but that a pK shift of the proton binding site upon translocation by at least 1.5 pK units is responsible for the apparent asymmetry of the transporter (Fig. 6 C). For this reason, we conclude that glutamate release at the intracellular side is controlled by a pK shift of a temporarily protonated amino acid residue in EAAC1.

The steep rise of the K_M value at pH 4.8 in the reverse transport mode of EAAC1 does not fit to the model developed above. At this nonphysiological low pH, the concentration of anionic glutamate is reduced only by 30% with respect to the protonated form. If EAAC1 bound only anionic glutamate, this minor reduction in anionic glutamate would not explain the dramatic decrease in the affinity of EAAC1 for glutamate. Billups and Atwell (1996) described for the glial transporters in Müller cells of salamander that, at low pH, protons compete with the extracellular sodium binding site, causing decreased glutamate-induced currents. Although in the pH range between 6.0 and 10.0 this effect was not observed for the neuronal glutamate transporter EAAC1, such a competitive effect at the intracellular Na^+ binding site would explain the behavior of EAAC1 at very low pH values of 4.8. Finally, high proton concentrations of ≈16 μM, pH 4.8, could directly affect the 3-D structure of the transporter, or the functional differences are related to surface charge effects, thus, dramatically changing the kinetic properties of EAAC1. At present, our data do not allow us to differentiate between these possibilities.

In the absence of permeant anions, the I_{max} value is unaffected by proton concentration. However, if inter-

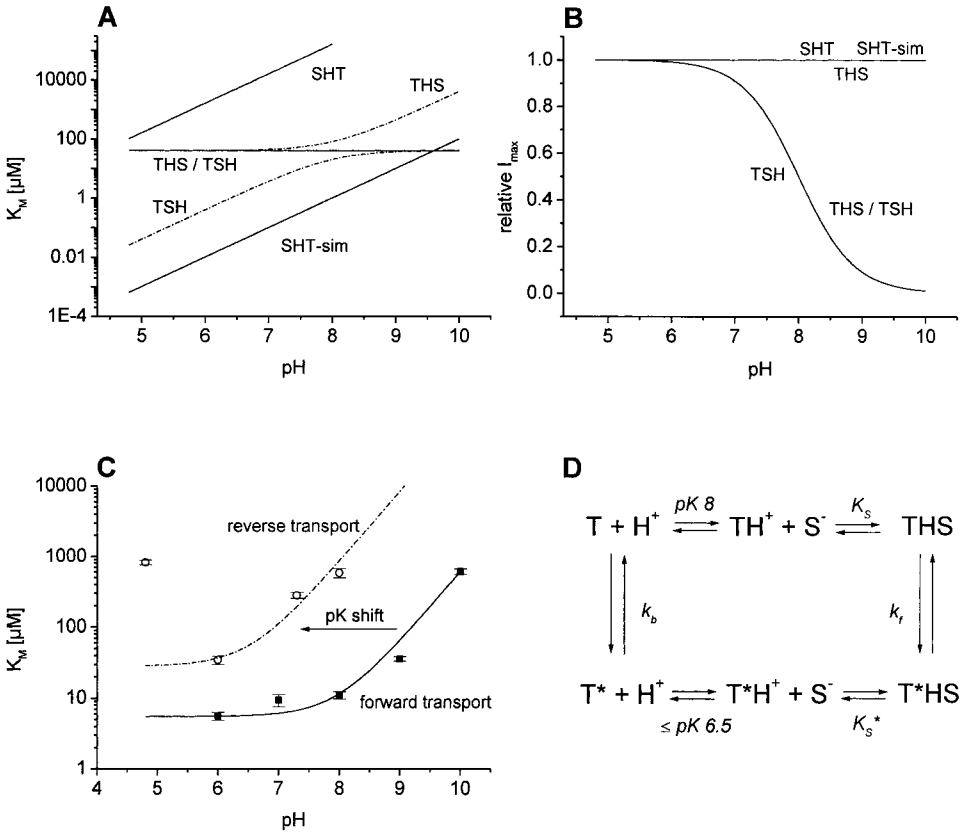

FIGURE 6. (A and B) Simulation of K_M and I_{max} for the five possible models. Parameters are as follows: dissociation constant for glutamate (K_S) 5.5 µM, pK of the ionizable amino acid residue in the transporter protein 8.0, pK of glutamate 4.4. (C) Semilogarithmic plot of the extracellular and intracellular K_M values at different pH values. The solid and dashed lines represent the fits $\{K_S(K_H + [H]/[H]\}$ to the model the (Table II), where first the proton binds to the transporter and is followed by the glutamate binding process. The parameters were set to the following values: extracellular K_M values (solid square), solid line, K_S 5.5 µM and K_H $1.1 \cdot 10^{-8}$ M, intracellular K_M (open circle), dotted line, K_S 28 µM and K_H $3.0 \cdot 10^{-7}$ M. (D) Kinetic model for glutamate transport by EAAC1. The empty transporter T first binds the proton H forming TH and afterwards binds glutamate S, under formation of the transporter-proton-glutamate complex THS. The respective states with their substrate binding sites exposed to the intracellular side are marked with an asterisk. K_S and K_S^* are the dissociation constants of glutamate from the extra- and intracellular site of EAAC1, respectively. k_f and k_b are the rate constants (forward mode) for translocation of the fully loaded carrier and relocation of the K^+-bound carrier, respectively.

nal SCN^- is present, an increase of I_{max} with decreasing pH was observed. This slight pH dependence of $I_{anionic}^{Glu^-}$ may in principle be caused by the following: (a) pH-sensitive rate constants for the transition to the anion-conducting state; (b) a proton dependence of the translocation rate of anions across the membrane; or (c) an additional proton flux through the transporter, such as the one activated by arachidonic acid (Fairman et al., 1998; Tzingounis et al., 1998), which might be caused by the permeant anion. In the first case, it is expected that the formation rate of the anion-conducting state, which is reflected by the rise of $I_{anionic}^{Glu^-}$, is pH-dependent. However, such a pH dependence of τ_{rise} was never observed in our kinetic experiments (Fig. 2). In the third scenario, the voltage dependence of the steady state $I_{anionic}^{Glu^-}$ should be affected by the pH because of the additional proton conductance imposed by the pH gradient. This was not observed either, ruling out this possibility as well. Therefore, we favor the second model. The pH dependence of $I_{anionic}^{Glu^-}$ is relatively shallow and shows no pronounced inflection point. We speculate that this behavior may be caused by the titration of surface charges of the EAAC1 protein (Fersht, 1999) that affect the anion translocation rate across the membrane. However, as we are not able to determine unitary anion conductance changes of EAAC1, it is not possible to further test this model.

The current–voltage relationship for EAAC1 in the reverse transport mode at physiological pH shows a weaker voltage dependence compared with the forward transport mode, indicating that other steps in the transport cycle with a different voltage dependence become rate limiting under these conditions (Fig. 4 D; Szatkowski et al., 1990; Noda et al., 1999). Substantial differences in the mechanism between forward and reverse transport have been observed before (Schwartz and Tachibana, 1990), however, the exact cause for this difference is unknown. It is unlikely that proton binding is rate limiting since I_{max} is not significantly affected by the pH. One could speculate that the transporter reaction steps that follow proton binding may be slowed down by the proton binding preequilibrium, which is shifted to the deprotonated form under physiological conditions.

The ordered proton–glutamate binding model (THS) developed from our experimental data provides further information about the question whether a proton or a OH^- is the pH-changing ion that is transported by EAAC1. The existence of a kinetic deuterium effect argues against OH^- countertransport. If OH^-

was countertransported, a kinetic isotope effect of extracellular deuterium should not be observed. Furthermore, the small mass ratio of 0.94 between OH^- and OD^- is not in agreement with such an effect. In contrast, kinetic isotope effects of ~1.5–3 are found for other proton translocating systems such as bacteriorhodopsin (le Coutre and Gerwert, 1996), the cytochrome *c* oxidase (Hallen et al., 1994; Ruitenberg et al., 2000), and the lactose permease (Viitanen et al., 1983). The major isotope effect is observed for the pre–steady state component of the current, whereas the steady state current is only slightly affected. We have proposed recently that the decay of the transient current component is closely associated with the glutamate translocation step, occurring within milliseconds (Grewer et al., 2000b). The isotope effects obtained here suggest that the proton is translocated together with glutamate in this early step in the transport cycle (Fig. 6 D). However, the steady state transport rate is limited by a later step in the EAAC1 reaction cycle, most likely the relocation of the K^+-bound transporter (Grewer et al., 2000b). The lack of a pronounced deuterium effect on the steady state turnover rate is consistent with this model. It should be noted here that our data do not rule out a secondary isotope effect, although these effects are typically smaller than the one observed here (Fersht, 1999).

How do our results compare to previous studies? It has been suggested that glutamate becomes protonated after it is bound to the transporter. This suggestion was questioned by Slotboom et al. (1999), referring to measurements of Mitrovic et al. (1998). The latter showed that L-serine-*O*-sulfate with a pK lower than 0 is a substrate for EAAT1 and 2. We also found for EAAC1 that L-serine-*O*-sulfate is transported by EAAC1 (data not shown). However, a rise in the pK of the bound L-serine-*O*-sulfate in the binding pocket of EAAC1 transporter, which is protonated at physiological pH values is unlikely, as it would require a proton affinity shift of $\approx 10^7$. Thus, the TSH model is not sufficient to explain the proton transport by glutamate transporters.

Apart from L-serine-*O*-sulfate, cysteine is accepted as a substrate of glutamate transporters (Zerangue and Kavanaugh, 1996b). Based on electrical and fluorescence measurements of *Xenopus* oocytes expressing EAAT3, Zerangue and Kavanaugh (1996a) proposed a model in which proton cotransport rather than a OH^- countertransport is associated with the glutamate translocation. These results are consistent with our data. These authors also suggested (Zerangue and Kavanaugh, 1996b) that cysteine is transported either as an anion or in the protonated form, as the affinity for cysteine (pK 8.3) did not change between pH 7.5 and 8.5, whereas the thiolate anion concentration increased 4.5-fold. In addition, the authors described a twofold increase in the K_M for glutamate at pH 6.5. If the anionic as well as the protonated form of cysteine are transported, this rise in K_M should not be detected. Furthermore, in line with the results obtained here for glutamate transport, the maximal transporter current did not change significantly with pH. These findings can be accounted for by the sequential proton–substrate binding mechanism presented here, assuming that the neutral, protonated form of the substrate is not transported. In this case, the K_M for cysteine increases at both low and high proton concentrations, and approaches a minimum around pH 8 as found experimentally (Zerangue and Kavanaugh, 1996b). It should be noted that our model also explains the lack of intracellular acidification upon cysteine transport (Zerangue and Kavanaugh, 1996a), in contrast to glutamate transport. Because of the relatively high pK, the majority of $cysteine^-$ ions will recombine with the cotransported proton once they dissociate from the transporter on the intracellular side, thus, buffering the translocated protons. Because of the low pK of glutamate this buffering process will not occur, leading to a pronounced decrease in intracellular pH mediated by glutamate transport.

Physiological Significance

Glutamate is stored in synaptic vesicles at a pH of 5–5.5 (Südhof, 1995; Miesenbock et al., 1998). After exocytosis, the acidic vesicle content is most likely rapidly buffered. Upon continuous synaptic stimulus, the extracellular pH shifts by ~0.1 U to basic values within a few tens of milliseconds (Gottfried and Chesler, 1996). Therefore, glutamate uptake will not be impaired by sustained synaptic transmission under physiological conditions because the transporter is quite insensitive to the extracellular pH in a range between 6.0 and 8.0. The pK difference between the intra- and extracellular proton binding sites strongly favors forward transport under normal physiological conditions. However, under pathophysiological conditions, as encountered in brain ischemia, the intra- and extracellular proton concentrations rise to ~1 μM, pH 6.0, (Mutch and Hansen, 1984; Silver and Erecinska, 1992). Thus, it is expected that in ischemic tissue, saturation of the internal proton binding site is induced, which would prompt EAAC1 to an increased probability of reverse transport. Reversed glutamate transport has been observed upon experimentally induced energy deprivation (Jabaudon et al., 2000; Rossi et al., 2000). Therefore, saturating intracellular proton concentrations may represent the main trigger of transporter-mediated glutamate release and excitotoxicity and, thus, could be a target mechanism to fight glutamate neurotoxicity.

We thank Drs. W. Schwarz and F. Weinreich for critical reading of the manuscript, M. Dumbsky for excellent technical assistance, and Dr. H. Wässle for continuous encouragement and support.

This work was supported by the Deutsche Forschungsgemeinschaft (grant No. GR 1393/2-1).

Submitted: 6 July 2000
Revised: 21 August 2000
Accepted: 22 August 2000

REFERENCES

Billups, B., and D. Atwell. 1996. Modulation of non-vesicular glutamate release by pH. *Nature.* 379:171–174.

Bouvier, M., M. Szatkowski, A. Amato, and D. Attwell. 1992. The glial cell glutamate uptake carrier countertransports pH-changing anions. *Nature.* 360:471–474.

Chen, C., and H. Okayama. 1987. High-efficiency transformation of mammalian cells by plasmid DNA. *Mol. Cell. Biol.* 7:2745–2752.

Eigen, M., and G.G. Hammes. 1963. Elementary steps in enzyme reactions. *In* Advances in Enzymology. F.F. Nord, editor. Wiley & Sons Inc., New York. 1–38.

Erecinska, M., D. Wantorsky, and D.F. Wilson. 1983. Aspartate transport in synaptosomes from rat brain. *J. Biol. Chem.* 258: 9069–9077.

Fairman, W.A., R.J. Vandenberg, J.L. Arriza, M.P. Kavanaugh, and S.G. Amara. 1995. An excitatory amino-acid transporter with properties of a ligand-gated chloride channel. *Nature.* 375:599–603.

Fairman, W.A., M.S. Sonders, G.H. Murdoch, and S.G. Amara. 1998. Arachidonic acid elicits a substrate-gated proton current associated with the glutamate transporter EAAT4. *Nat. Neurosci.* 1:105–113.

Fendler, K., E. Grell, M. Haubs, and E. Bamberg. 1985. Pump currents generated by the purified Na^+K^+-ATPase from kidney on black lipid membranes. *EMBO (Eur. Mol. Biol. Organ.) J.* 4:3079–3085.

Fersht, A. 1999. Structure and Mechanism in Protein Science. W.H. Freeman and Company, New York. 169–188.

Gottfried, J.A., and M. Chesler. 1996. Temporal resolution of activity-dependent pH shifts in rat hippocampal slices. *J. Neurophysiol.* 76:2804–2807.

Grewer, C. 1999. Investigation of the α1-glycine receptor channel-opening kinetics in the submillisecond time domain. *Biophys. J.* 77:727–738.

Grewer, C., J. Jäger, B.K. Carpenter, and G.P. Hess. 2000a. A new photolabile precursor of glycine with improved properties: a tool for chemical kinetic investigations of the glycine receptor. *Biochemistry.* 39:2063–2070.

Grewer, C., N. Watzke, M. Wiessner, and T. Rauen. 2000b. Glutamate translocation of the neuronal glutamate transporter EAAC1 occurs within milliseconds. *Proc. Natl. Acad. Sci. USA.* 97: 9706–9711.

Hallen, S., P. Brzezinski, and B.G. Malmstrom. 1994. Internal electron transfer in cytochrome c oxidase is coupled to the protonation of a group close to the bimetallic site. *Biochemistry.* 33:1467–1472.

Hamill, O.P., A. Marty, E. Neher, B. Sakmann, and F.J. Sigworth. 1981. Improved patch-clamp techniques for high-resolution current recording from cells and cell-free membrane patches. *Pflugers Arch.* 391:85–100.

Hess, G.P. 1993. Determination of the chemical mechanism of neurotransmitter receptor-mediated reactions by rapid chemical kinetic techniques. *Biochemistry.* 32:989–1000.

Jabaudon, D., M. Scanziani, B.H. Gähwiler, and U. Gerber. 2000. Acute decrease in net glutamate uptake during energy deprivation. *Proc. Natl. Acad. Sci. USA.* 97:5610–5615.

Kanai, Y., and M.A. Hediger. 1992. Primary structure and functional characterization of a high-affinity glutamate transporter. *Nature.* 360:467–471.

Kandel, E.R., J.H. Schwartz, and T.M. Jessell. 1995. Essentials of Neural Science and Behavior. Appleton & Lange, East Norwalk, CT. 225–248.

Kanner, B.I., and I. Sharon. 1978. Active transport of L-glutamate by membrane vesicles isolated from rat brain. *Biochemistry.* 17: 3949–3953.

le Coutre, J., and K. Gerwert. 1996. Kinetic isotope effects reveal an ice-like and liquid-phase-type intramolecular proton transfer in bacteriorhodopsin. *FEBS Lett.* 398:333–336.

Mennerick, S., W. Shen, W. Xu, A. Benz, K. Tanaka, K. Shimamoto, K.E. Isenberg, J.E. Krause, and C.F. Zorumski. 1999. Substrate turnover by transporters curtails synaptic glutamate transients. *J. Neurosci.* 19:9242–9251.

Miesenbock, G., D.A. De Angelis, and J.E. Rothman. 1998. Visualizing secretion and synaptic transmission with pH-sensitive green fluorescent proteins. *Nature.* 394:192–195.

Milburn, T., N. Matsubara, A.P. Billington, J.B. Udgaonkar, J.W. Walker, B.K. Carpenter, W.W. Webb, J. Marque, W. Denk, et al. 1989. Synthesis photochemistry and biological activity of a caged photolabile acetylcholine receptor ligand. *Biochemistry.* 28:49–56.

Mitrovic, A.D., S.G. Amara, G.A. Johnston, and R.J. Vandenberg. 1998. Identification of functional domains of the human glutamate transporters EAAT1 and EAAT2. *J. Biol. Chem.* 273: 14698–14706.

Mutch, W.A., and A.J. Hansen. 1984. Extracellular pH changes during spreading depression and cerebral ischemia: mechanisms of brain pH regulation. *J. Cereb. Blood Flow Metab.* 4:17–27.

Nelson, P.J., G.E. Dean, P.S. Aronson, and G. Rudnick. 1983. Hydrogen ion cotransport by the renal brush border glutamate transporter. *Biochemistry.* 22:5459–5463.

Niu, L., C. Grewer, and G.P. Hess. 1996. Chemical kinetic investigations of neurotransmitter receptors on a cell surface in the ms time region. *In* Techniques in Protein Chemistry VII. D.R. Marshak, editor. Academic Press, Inc., New York. 133–149.

Noda, M., H. Nakanishi, and N. Akaike. 1999. Glutamate release from microglia via glutamate transporter is enhanced by amyloid-beta peptide. *Neuroscience.* 92:1465–1474.

Otis, T.S., and C.E. Jahr. 1998. Anion currents and predicted glutamate flux through a neuronal glutamate transporter. *J. Neurosci.* 18:7099–7110.

Otis, T.S., and M.P. Kavanaugh. 2000. Isolation of current components and partial reaction cycles in the glial glutamate transporter EAAT2. *J. Neurosci.* 20:2749–2757.

Rauen, T., J.D. Rothstein, and H. Wassle. 1996. Differential expression of three glutamate transporter subtypes in the rat retina. *Cell Tissue Res.* 286:325–336.

Rossi, D.J., T. Oshima, and D. Attwell. 2000. Glutamate release in severe brain ischemia is mainly by reverse uptake. *Nature.* 403: 316–320.

Ruitenberg, M., A. Kannt, E. Bamberg, B. Ludwig, H. Michel, and K. Fendler. 2000. Single-electron reduction of the oxidized state is coupled to proton uptake via the K pathway in *Paracoccus denitrificans* cytochrome c oxidase. *Proc. Natl. Acad. Sci. USA.* 97:4632–4636.

Schwartz, E.A., and M. Tachibana. 1990. Electrophysiology of glutamate and sodium co-transport in a glial cell of the salamander retina. *J. Physiol.* 426:43–80.

Silver, I.A., and M. Erecinska. 1992. Ion homeostasis in rat brain in vivo: intra- and extracellular $[Ca^{2+}]$ and $[H^+]$ in the hippocampus during recovery from short-term, transient ischemia. *J. Cereb. Blood Flow Metab.* 12:759–772.

Slotboom, D.J., W.N. Konings, and J.S. Lolkema. 1999. Structural features of the glutamate transporter family. *Microbiol. Mol. Biol.*

Rev. 63:293–307.

Südhof, T.C. 1995. The synaptic vesicle cycle: a cascade of protein-protein interactions. *Nature.* 375:645–653.

Szatkowski, M., B. Barbour, and D. Attwell. 1990. Non-vesicular release of glutamate from glial cells by reversed electrogenic glutamate uptake. *Nature.* 348:443–446.

Tzingounis, A.V., C.L. Lin, J.D. Rothstein, and M.P. Kavanaugh. 1998. Arachidonic acid activates a proton current in the rat glutamate transporter EAAT4. *J. Biol. Chem.* 273:17315–17317.

Viitanen, P., M.L. Garcia, D.L. Foster, G.J. Kaczorowski, and H.R. Kaback. 1983. Mechanism of lactose translocation in proteoliposomes reconstituted with lac carrier protein purified from *Escherichia coli.* 2. Deuterium solvent isotope effects. *Biochemistry.* 22: 2531–2536.

Wadiche, J.I., and M.P. Kavanaugh. 1998. Macroscopic and microscopic properties of a cloned glutamate transporter/chloride channel. *J. Neurosci.* 18:7650–7661.

Wadiche, J.I., S.G. Amara, and M.P. Kavanaugh. 1995a. Ion fluxes associated with excitatory amino acid transport. *Neuron.* 15:721–728.

Wadiche, J.I., J.L. Arriza, S.G. Amara, and M.P. Kavanaugh. 1995b. Kinetics of a human glutamate transporter. *Neuron.* 14:1019–1027.

Walker, J.W., G.P. Reid, J.A. McCray, and D.R. Trentham. 1988. Photolabile 1-2 nitrophenylethyl phosphate esters of adenine nucleotide analogues synthesis and mechanism of photolysis. *J. Am. Chem. Soc.* 110:7170–7177.

Wieboldt, R., K.R. Gee, L. Niu, D. Ramesh, B.K. Carpenter, and G.P. Hess. 1994. Photolabile precursors of glutamate: synthesis, photochemical properties, and activation of glutamate receptors on a microsecond time scale. *Proc. Natl. Acad. Sci. USA.* 91:8752–8756.

Zerangue, N., and M.P. Kavanaugh. 1996a. Flux coupling in a neuronal glutamate transporter. *Nature.* 383:634–637.

Zerangue, N., and M.P. Kavanaugh. 1996b. Interaction of L-cysteine with a human excitatory amino acid transporter. *J. Physiol.* 493:419–423.

Zhang, Y., G. Pines, and B.I. Kanner. 1994. Histidine 326 is critical for the function of GLT-1, a (Na^{++} K^{+})-coupled glutamate transporter from rat brain. *J. Biol. Chem.* 269:19573–19577.